Energy 140.1 (2017): 682-695

**DOI:** https://doi.org/10.1016/j.energy.2017.08.113

# INTEGRATING LONG-TERM ECONOMIC SCENARIOS INTO PEAK LOAD FORECASTING: AN APPLICATION TO SPAIN

Julián Moral-Carcedo (*)

Dpto. An. Económico: Tª Económica
Universidad Autónoma de Madrid

Julián Pérez-García (**)

Dpto. Economía Aplicada
Universidad Autónoma de Madrid

(*) Corresponding author. E-mail: julian.moral@uam.es Universidad Autónoma de Madrid. Fac. CC. Económicas. Campus de Cantoblanco. Madrid 28049. Spain.

(**)E-mail: julian.perez@uam.es Universidad Autónoma de Madrid. Fac. CC. Económicas. Campus de Cantoblanco. Madrid 28049. Spain.

## Abstract

The treatment of trend components in electricity demand is critical for long-term peak load forecasting. When forecasting high frequency variables, like daily or hourly loads, a typical problem is how to make long-term scenarios - regarding demographics, GDP growth, etc. - compatible with short-term projections. Traditional procedures that apply de-trending methods are unable to simulate forecasts under alternative long-term scenarios. On the other hand, existing models that allow for changes in long-term trends tend to be characterized by end-of-year discontinuities. In this paper a novel forecasting procedure is presented that improves upon these approaches and is able to combine long and short-term features by employing temporal disaggregation techniques. This method is applied to forecast electricity load for Spain and its performance is compared to that of a nonlinear autoregressive neural network with exogenous inputs. Our proposed procedure is flexible enough to be applied to different scenarios based on alternative assumptions regarding both long-term trends as well as short-term projections.

*JEL classification:* Q4, L94, C53

*Keywords:* Peak load forecasting, load curve forecasting, long-term scenarios, temporal disaggregation

*Highlights:*

Grid capacity planning is critically linked to peak demand forecasts.

A methodology to produce long-term hourly peak load forecasting is presented.

Modelling hourly load have to deal with long-term and short-term features.

Long and short-term features are combined by temporal disaggregation techniques.

The method is flexible and allows for what-if simulations, key in grid planning.

# 1. INTRODUCTION

Long-term peak and trough load forecasts are key in the generation and transmission planning process for non-storable utilities like electricity. Grid capacity has to be dimensioned adequately in order to meet the requirements of the hourly/ type-of-day/ monthly/ yearly variable demand which characterizes the electricity market. In particular, grid capacity is critically linked to peak demand, and security margins have to be adapted with enough anticipation to deal with uncertain variations in demand. Inaccurate forecasts can lead to costly access capacity and/or the risk of overcharging the electric power system.

Regarding short-term load forecasting, recent models based on Artificial Neural Networks, Genetic Algorithms, and Support Vector Machines have shown to work relatively well. For instance, Che and Wang (2014) [1] propose a combination of kernel-based support vector regressions (SVR) and are able to quite accurately forecast half-hour electricity loads in California, for a horizon of up to 15 days and using training samples of 26 day-data. Yang et al. (2016) [2] use a method that is also based on SVRs, but their model is trained with a shorter sample and is continuously re-trained with new data. In their application the authors use a training sample of 3 days of half-hour electricity load data, which is re-trained with 2 day-data in order to make predictions for a 15-days horizon. A combination of SVRs and a multiple linear regression model is proposed by Che (2014) [3]. His hybrid model is trained with 29 days of hourly data, and its forecasting accuracy is tested by launching predictions for a period of 24 hours. Dedinec et al. (2016) [4] propose a neural network model (deep belief network) to forecast hourly electricity consumption (24-hours ahead). Forecasting total consumption, the authors are able to obtain a considerably low value (3.3%) for the mean absolute percentage error (MAPE). Badurally Adam et al. (2011) [5] model monthly peak electricity demand in Mauritius using Gross domestic product (GDP) and weather factors such as temperature, hours of sunshine, and humidity as explanatory variables in a Gompertz diffusion process where coefficients are estimated by a genetic algorithm.

Although short-term forecasting (i.e. for a horizon of less than 15 days) is key for grid operation, in the current paper a long term load forecasting perspective is adopted. As pointed out in Hahn et al. (2009) [6], due to the progressive deregulation of the electricity market, literature is paying increasingly more attention to load forecasts with longer time-horizons. Because grid capacity investments require long term planning which needs demand forecasts at a multi annual basis, as remarked in Zhao and Guo (2016) [7]. However, investment planning not only requires annual power load forecasts. These large-scale investments (e.g. in Spain they amount to 4,700 million Euros for 2014-2019.) also have to guarantee adequate grid security margins and hence also expected intraday variability in demand has to be considered. This requires combining hourly with long term load forecasts. The current paper proposes a methodology that allows to obtain accurate long-term forecasts of electricity loads at hourly frequencies. Motivated by the need for long-term grid capacity planning, the proposed methodology is based on multiple linear regression models which allows to account for different scenarios regarding the effect of exogenous variables like economic activity, or outside temperatures on electricity demand. This flexibility is key, because for grid planning it is not only important to obtain accurate projections

for one specific scenario, but also to be able to infer the width of the security margin if economic or environmental and weather conditions differs from expected.

Usually in electricity consumption forecasting for long-term and short-term horizons are viewed as two distinct objects. As Dedinec et al. (2016) [4] points out, the main difference between both types of predictions lies with the variables that affect electricity demand at different time horizons. Peak load forecasting for the long-run requires to consider factors that influence electricity demand both in the long and a short run. In Nedellec et al. (2014) [8] electricity load is modelled by means of three additive components, each reflecting long, medium and short patterns respectively. Typical long-term factors affecting electricity demand are demographic change, variations in economic activity, substitution effects between energy sources, adoption of more efficient technologies, and mechanization/automatization of production processes. These factors have to be combined with short-term features, such as weekday effects, yearly cycle of temperature variations, or time-of-day demand (opening hours) as pointed out in Taylor (2010) [9] and Mestekemper et al. (2013) [10]. The ideal forecasting procedure does not only model these long and short term factors adequately in isolation, but is also able to integrate them.

Models that tend to work well for short-term projections based on, Support Vector Machines, ARIMA methodology, or Neural Networks (used as a comparison method to ours in Section 3.1.1 ) usually perform very poorly when used for long-term forecasting (i.e.. for monthly or yearly horizons). This is due to the fact that these models are unable to capture breaks in trend movements, and hence unless combined with other methods, they result inadequate for forecasts of electricity loads under alternative long-term scenarios. Certain particularities regarding long-term electricity consumption make it more convenient to analyze it separately from short-term developments. One of the reasons is that in the long run, electricity consumption reflects the changing nature of the electricity-economic growth nexus, due to technological progress, advances in energy efficiency, changes in consumer behavior, etc. Previous works, like [11], show that reasonable long term annual forecasts can be obtained by exploiting the strong correlation between electricity consumption and economic variables like Gross Domestic Product, GDP per capita, and population.

All the above mentioned studies highlight the important differences between the long and short-term behavior of electricity demand, and hence they point to the need for both aspects to be analyzed alongside each other. Previous works focusing on long-term peak forecasting propose different ways to deal with factors affecting electricity demand at different time horizons. Cho et al. (2013) [12] propose to model the overall trend and seasonality of electricity demand by fitting a generalized additive model to weekly averages of electricity load. To model short-term features and the dependency among the daily loads authors propose a curve linear regression model. Other authors [13] propose to subtract the “trend-seasonal” component from the electricity load and to model it separately. After de-trending the original series, short-term characteristics such as temperature effect, working-day effect, etc. are then modelled by means of casual regression analysis, ARIMA, or Neural Networks. However, typical de-trending methods like the ones mentioned above are only valid locally, and hence these models do not perform well when sudden changes in trend occur, or when the forecasting period is far from the sample period used for parameter estimation. Hyndman and Fan (2010) [13] on the other hand suggest to explicitly model the long-term characteristics of electricity consumption within a low frequency model

(using annual data), assuming that these characteristics remain constant during any intra-year periods. The main advantage of this procedure is that it allows to control for changes in demographic variables (population, number of households, etc.), variations in economic variables (GDP, per household income, price of electricity and other energy sources etc.), as well as technological progress (usually by means of different time trends); factors which all matter for long-term modelling and forecasting of energy demand. The problem with this procedure is that due to the assumption that long-term characteristics remain constant during intra-year periods, forecasts at the beginning of each year are characterized by discontinuities. Moreover, a procedure that only allows for changes in the trend component at the end of each year might affect the estimated temperature effect[1]. A different approach as proposed by Nedellec et al. (2014) [8] models the long-term component of the half hour load curve by adjusting a Gaussian kernel to monthly electricity load data (adding seasonal and temperature effects). The authors then linearly interpolate the estimated trend to obtain half-hour estimates, and using simple constant extrapolation they are able to make forecasts at weekly horizons. However, the use of a constant extrapolation of the trend limits the scope of this method to short-term forecasts only.

In this paper a novel procedure is presented that improves upon these existing methods. By applying temporal disaggregation techniques it is possible to obtain high frequency estimates (daily) of the long-term component These estimates are used together with other variables like temperature and weekday effects, and daylight duration to model the high frequency behavior of electricity consumption (hourly demand). This approach allows to build a causal model for peak demand, i.e. maximum hourly consumption for a given period (week, month, or year) and trough demand, i.e., minimum hourly consumption for the same period. Using different long-term scenarios and varying assumptions regarding short-term factors, the model is used to obtain long-term forecasts for peak and trough demand for Spain. The remainder of this paper is organized as follows: In the following section a description of this methodology is provided. In Section 3 the model's performance is analyzed. Finally, Section 4 concludes.

## 2. MODELLING STRATEGY

The dynamics of electricity loads exhibit both low and high frequency features that have to be taken into account in order to develop an adequate forecasting model. In particular, as Figure 1 shows, long-term developments have an important impact on electricity demand in Spain. Between 1996 and 2007, hourly peak and trough loads nearly doubled - they increased by 1.77 and 1.95 times respectively. But since the 2008 economic crisis, peak and trough loads have decreased by 14% and 2% respectively. Similarly, the grid stress (the difference between peak and trough loads) which indicates the capacity that has to be installed to meet demand without shortages in a given year, increased between 1996 and 2007 by 66%, but has decreased since

[1] Only allowing for changes in trend at the end of each year mechanically generates a discontinuity in electricity demand in January. This discontinuity can affect the estimated effect of winter (summer) temperatures on electricity demand.

2007 by 22%. Neither temperature nor climate variables, nor calendar effects, nor other high frequency variables are able to explain this huge increase in peak and trough loads, nor the 2008 turning point. These observations highlight the importance of taking into account long-term developments and to adequately model variables that affect the long-term evolution of electricity demand, in particular as they differ from other variables that have mainly short-term effects.

Figure 1.-Annual peaks and troughs of hourly electricity loads (MWh). Spain. 1996-2014

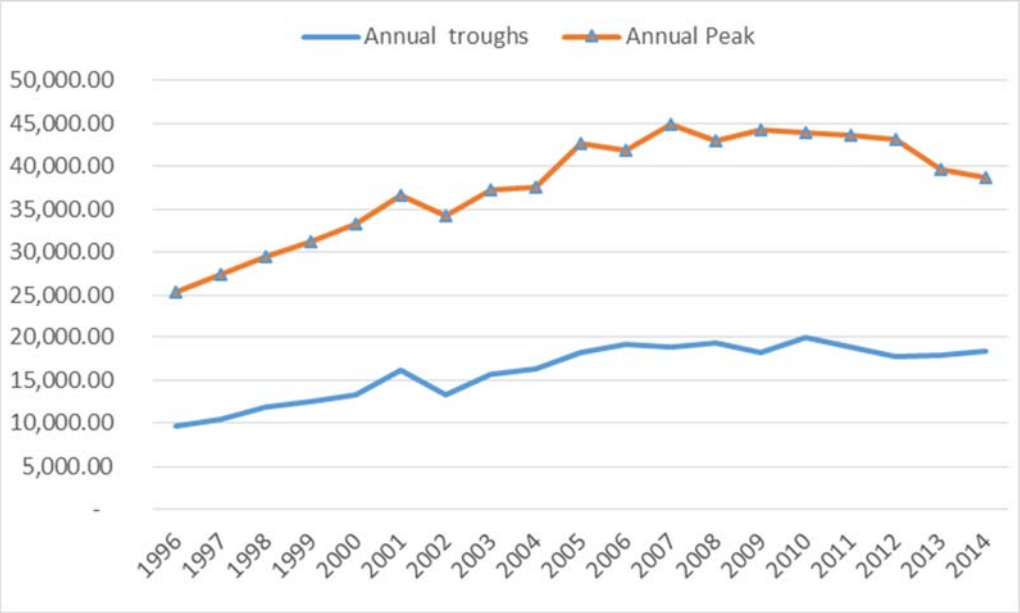


Source: Own elaboration with data from REE (Red Eléctrica de España S.A.)

Among variables that affect high frequency electricity loads are typical features of a country's economic activities, in particular as they relate to the usage of electricity during the day and within a year. Intraday changes in electricity demand reflect the beginning, breaks, and end of the working day. In Spain, the typical working day is remarkable different from those in other European countries. Figure 2 displays the share of people aged 20-74 working or studying at each hour on a typical work day in Spain and Germany. One can observe that working days in Spain start and end later and are characterized by a longer lunch break. In particular, the working day in Spain usually starts around 9-10 am and lasts until 8-9 pm (with a lunch break inactivity spell between 2-4 pm). The same pattern can be observed in electricity load curves both during summer and winter time; see Figure 3. In Spain, during winter (December-February) the typical peak load occurs on a "central" working day (Tuesday-Thursday) around 7-9 pm. The peak in the summer shares similar features, but occurs at a different time of day, at 1-3 pm[2]. The lowest consumption hour typically correspond to a nonworking day (national holiday or weekend) between 5 pm and 9 am. However, these intra-day features are not the only variables that affect high frequency electricity loads. Because the cycle of economic activity interacts with daylight duration which in turn is also related to the temperature yearly cycle. As temperatures and daylight duration are also related, it is very difficult to disentangle each individual effect. Spain's

[2] In Spain it is very common to concentrate work days during the summer; i.e. from 7 am-3 pm.

coordinates (latitude and longitude) and daylight saving time clock shifts imply that in the course of a year the sun rises between 6.40 am and 8.38 am, while sunset occurs between 5.48 pm and 9.49 pm. Hence, in Spain economic activity usually starts with solar light and from October to March it ends with artificial light.

Figure 2 .- Share of people (20-74 years) "Working or Studying" during the day.

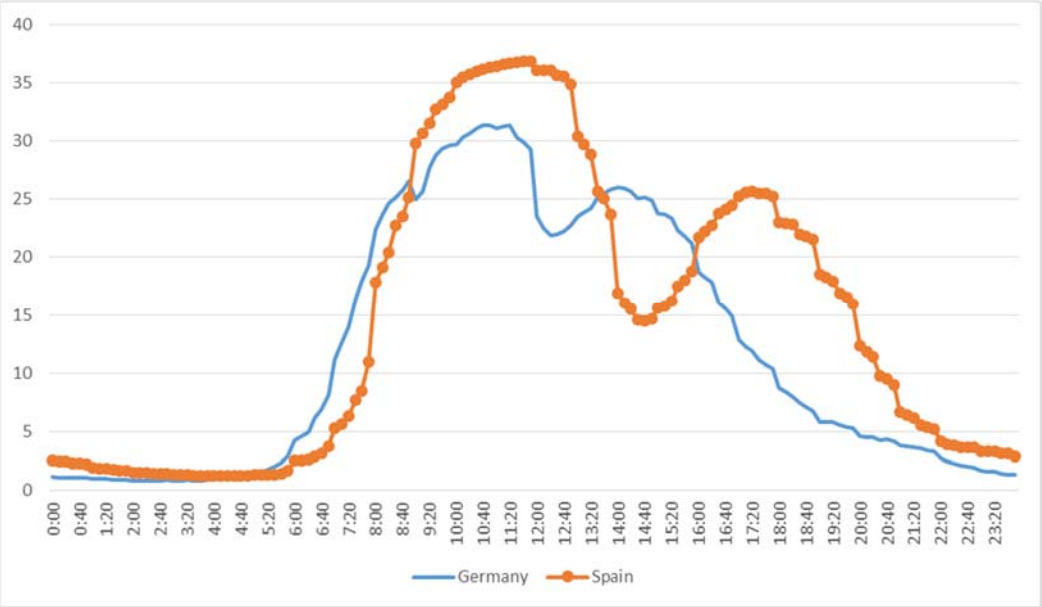


Source: Harmonised European Time Use Survey (2000)

Figure 3. – Peak and valley electricity loads for a typical working day in Spain.

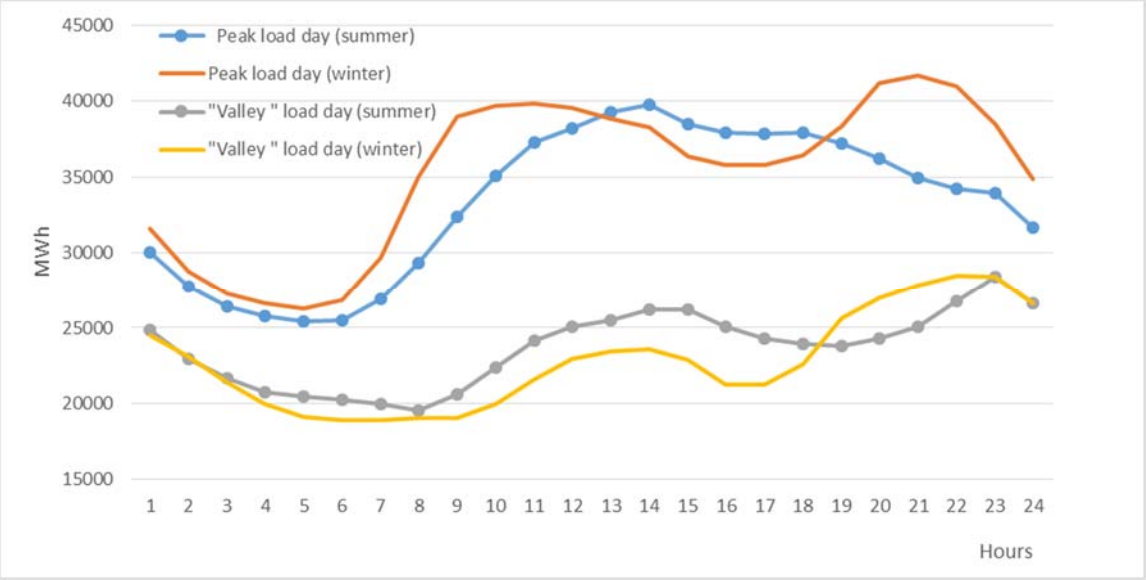


Source: Own elaboration with data from REE (Red Eléctrica de España S.A.)

The methodology proposed combines both these long and short-term drivers of electricity loads to generate long-term forecasts of hourly electricity demand. On the one hand, annual forecasts of electricity demand obtained from a long-term demand model (LTDM) converted to daily frequencies are employed. On the other hand, hourly demand forecasts are obtained by combining the LTDM forecasts at daily frequencies with working day and temperature effects that are estimated using hourly data. This procedure allows to generate hourly load curves under alternative scenarios characterized by different assumptions about economic activity (from the LTDM model) and temperatures (working day patterns are considered invariant). Once a load curve is generated, the extreme values (peaks and troughs) for any period of analysis - week, month, year- can easily be determined.

In particular, and similar to [13] and [14], the hourly load curve is modelled hour-by-hour and explanatory variables are allowed to have different effects on electricity demand at each hour of the day:

$$c_{i,t} \Rightarrow \begin{cases} c_{1,t} = \varphi_1(LF_t, HF_t) + \varepsilon_{1,t} \\ c_{2,t} = \varphi_2(LF_t, HF_t) + \varepsilon_{2,t} \\ \vdots \\ c_{24,t} = \varphi_{24}(LF_t, HF_t) + \varepsilon_{24,t} \end{cases} \qquad \text{[eq.1]}$$

where $c_{i,t}$ is electricity consumption at hour *i* on day *t*, $LF_t$ is the low frequency component (trend effect) and $HF_t$ is the high frequency component of electricity demand (calendar, temperature and daylight effect). $\varepsilon_{i,t}$ is the error term. Both the low frequency component as well as the high frequency component potentially have different effects at each hour, as indicated by the function $\varphi$ i(..) which is assumed to be linear.

Given the complexity of the calendar and temperature effects and their interaction, residuals in Equation 1 are likely to exhibit some degree of auto- and cross correlation. In addition, we assume that coefficients assigned to calendar and temperature effects remain constant over a fairly long period (1996-2014). If the weekly cycle or temperature effects evolves over time (e.g. due to increased flexibility in opening hours on Sundays, higher penetration of air-conditioning equipment, etc.) this can also lead to residual correlation (in Section 3 this aspect is analyzed in greater detail). However, the model's main purpose is to provide forecasts, and hence estimating precise coefficients for the function $\varphi$ i(..) is not the main interest.[3]

In order to be able to apply our methodology, the following issues have to be addressed: (1) Estimation of the low-frequency component. A long-term forecasting model is proposed, and the method used to transform annual demand forecasts into daily data is presented. (2) Estimation of the high-frequency component. Section 2.2 details how the high frequency features, such as

[3] As we include the same regressors in all equations, our OLS estimates are equivalent to SURE (Seemingly Unrelated Regressions) estimates, and thus we implicitly take into account any residual correlation among the equations.

working day and temperature effects using hourly data, are modelled, and how we account for the effects of daylight duration. (3) Finally, in Section 2.3 the model for hourly demand is specified.

## 2.1. LOW-FREQUENCY COMPONENT

The starting point for estimating the low-frequency component ($LF_t$) is an annual electricity demand model Annual data is chosen because for Spain detailed sectorial electricity consumption is only available on an annual basis. The data come from the Spanish system operator, Red Eléctrica de España (REE hereafter) which collects and homogenizes the information available from the Ministry of Industry, Energy, and Tourism. As mentioned before, the long-term behavior of electricity demand reflects the changing nature of the electricity-economic growth nexus driven by economic and technological factors. Previous work by Pérez-García and Moral-Carcedo (2016) [15] shows that the long-term behavior of electricity demand in Spain reflects marked differences between residential and non-residential demand. In order to better capture such long-term developments, electricity demand is modelled for both sectors separately. To this end, the methodology detailed in [15] is applied. The design of the proposed long-term forecasting model starts with Equation 2 which specifies that total demand ($C_T$) in year *T* can be obtained by adding up the specific consumption of each sector ($C_{i,T}$).

For non-residential sectors (i=1…S-1), electricity consumption can be obtained by multiplying total value added ($Y_{i,T}$) by the sector-specific intensity of electricity use ($I_{i,T}$). Residential electricity consumption can be computed as the number of households ($H_T$) multiplied by residential intensity ($I_{H,T}$).

$$C_T = \sum_{i=1}^{S} C_{i,T} = \sum_{i=1}^{S-1} Y_{iT} I_{i,T} + H_T I_{H,T} \qquad \text{[eq.2]}$$

For the purpose of the model, both the breakdown of GVA (Gross Value Added) by sector as well as the number of households are considered exogenous. These variables define the socio-economic environment that affects the future demand for electricity. The general structure of the Long-term Demand Model (LTD Model) is depicted in Figure4. To model long-term electricity demand the intensities of electricity use are defined as functions of three variables:

- The amount of total equipment, both in the productive sectors as well as in households that are powered by electricity.
- The efficiency and/or electrification factor, which includes both the share of total equipment powered by electricity (electrification) and the unitary consumption of this equipment (efficiency).
- The substitution effect that accounts for changes in electricity demand induced by changes in the relative price of electricity compared to alternative sources of energy (gas, fuel, etc.)

Figure 4 . General Structure of the Long Term Demand Model (LTDM)

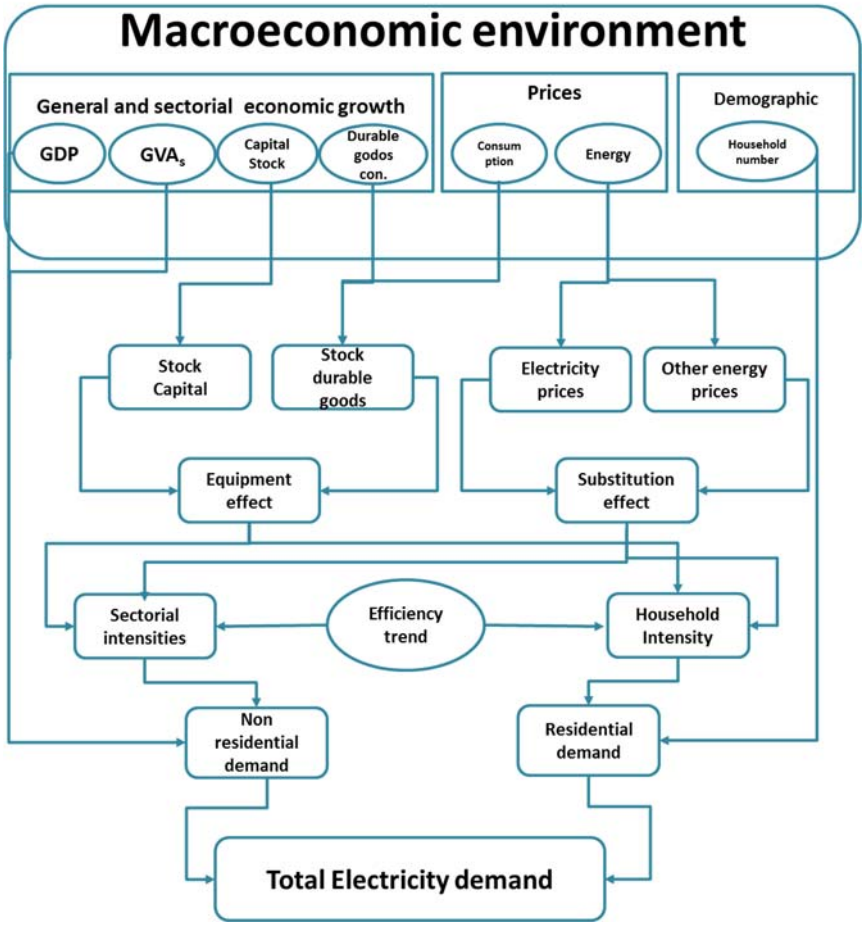


Source: Authors' own elaboration

The LTD model provides us with a baseline estimate for long-term electricity demand or the trend component. This trend aims to capture the long-term behavior of electricity consumption and it is a central input to our forecasting model. However, total demand generated by the LTD model comes at annual frequencies, making it necessary to break these series down into daily frequencies that are consistent with annual demand. To this end the Boot-Feibes and Lisman (BFL) disaggregation method proposed originally by Boot et al. (1967) [16] is considered. The main advantage of this method is that no additional indicators are needed - as is the case for instance when using the Chow-Lin procedure - nor does it require any assumptions regarding the underlying data generating process of the estimated trend. A drawback of this method is that is requires the inversion of matrices making it a computationally costly method in particular when dealing with large data samples.

Temporal disaggregation problems consist in estimating an unobserved series, in our case a daily series $y = \{y_{t,T} : t = 1,...,365/366; T = 1,...,N\}$ which is coherent with an observed annual series $Y = \{Y_T : T = 1,...,N\}$. Coherency implies that the longitudinal constraint is satisfied, $\sum_{t=1}^{365/366} y_{t,T} = Y_T \quad \forall T$, or in matrix form, $By = Y$, where $B = I_N \otimes f$, and where $f$ is a row vector of ones of size (1x 365/366).

The BFL method consists in estimating $y_{t,T}$ as the solution of a constrained minimization program in which the disaggregated series satisfies the longitudinal constraint and exhibits a smooth shape; i.e. $y_{t,T}$ solves

$$\text{Min} \sum_{i=2}^{M} (y_I - y_{I-1})^2 \quad i = 1,...,M; \qquad \text{[eq.3]}$$

$$\text{subject to} \sum_{t=1}^{365/366} y_{t,T} = Y_T \quad \forall T \qquad \text{[eq.4 ]}$$

where $M$ is the total number of days in the analyzed sample, taking into account if the year has 365 or 366 (leap year) days.

On the other hand, the computationally simpler quadratic match sum method requires solving the following equation

$y = at^2 + bt + c$ ; t=0,1,2,,..., 365/366

$$\text{subject to the longitudinal constraint} \sum_{t=1}^{365/366} y_{t,T} = Y_T \quad \forall T \qquad \text{[eq.5]}$$

Both procedures provide with daily values for the long-term trend (observed or predicted). However, the quadratic match sum method will generate discontinuities at the end of each year. This holds true in particular if no additional constraints are imposed (e.g. that the last daily data point estimated for a year has to equal the first one estimated for the following year). Especially when the series to model exhibits volatile changes in trend growth rates as is the case for electricity consumption in Spain after the 2008 crisis, the BFL method is much more reliable.

Furthermore, the BFL method has an additional advantage. The outcome of this method is similar to the one obtained when applying the widely used Hodrick-Prescott filter to the daily series of electricity consumption (with λ= 133,225,000). Although results for the two methods are very similar, there is an important difference when making forecasts. When using Hodrick Prescott filtered series, forecasts implicitly assume that trends follow an underlying IMA(2,1) process. Hence, the so-forecasted values can exhibit notorious inertia, typical for dynamic non-casual models. In the BFL trend estimation on the other hand, the forecasted values are derived from a causal model (LTD model) which is expressed in annual terms. In addition, annual values for electricity consumption under different scenarios regarding electricity demand can be generated ("what-if "simulations). The BFL approach thus offers greater flexibility for simulating alternative scenarios, something that is essential in the generation and transmission planning process for non-storable utilities like electricity.

## 2.2. HIGH FREQUENCY COMPONENT

For the high frequency component of the model the following three effects are considered: calendar effect, temperature effect, and daylight duration.

### 2.2.1. Calendar effect

Daily electricity demand is strongly affected by weekly cycles and calendar effects. As pointed out in Che (2014) [3] intraweek and intraday seasonal cycles heavily condition short-term profiles of electricity loads. Also the intra annual variation of temperatures translates into an intra annual cycle in electricity loads as pointed out by [17]. Although such cycles can show up differently in the electricity demand of different economic sectors, as reflected in [18], a common aggregate pattern can be observed. In particular, the repeated succession of working days and weekends creates an underlying periodic 7-day behavior, only interrupted by holidays and other deterministic events (national strikes, etc.). The high frequency components of the load curves are mainly driven by such weekly cycles. Another calendar effect that has to be taken into account is the month effect, i.e. seasonality not explained for by variations in temperature. The month effect is particularly important during summer holidays, but a priori it cannot be ruled out that it could also be significant for other months.

Given that the main purpose of the model is to provide reliable forecasts, a causal specification that is able to deal with calendar effects is proposed. The main advantage of this specification is the off-sample treatment of non-periodic features of calendar effects (holidays, Easter week, leap year, etc.) which are hard to capture using dynamic models.

The following model for estimating calendar effects is defined,

$$f_i(D_t) = \beta_{0i} + \sum_{j=1}^{f} \beta_{ji} D_{jt} + \sum_{k=f+1}^{f+11} \beta_{ki} M_{k-f,t} \qquad \text{[eq.6]}$$

where $D_{jt}$ is a dummy variable that takes on value 1 whenever day $t$ belongs to type $j$ ( $j$ =1,2,.. $f$ with $f$=1,..,182 detailed in Table 1 ), $\beta_{ji}$ is the effect of day type $j$ on electricity load at hour $i$ (i=1,…24,.), $\beta_{ki}$ is the effect of month $M_{k\text{-}f,t}$ ($k$=1,…11) on electricity load at hour $i$ (seasonality), $M_{k\text{-}f,t}$ is a dummy variable taking on value 1 if day $t$ belongs to month $k$. The reference value $\beta_{0i}$ is a Wednesday in January.

Other effects linked to the calendar that are also included in our model are general strikes and dummy variables indicating if the last day in July is a Monday, Tuesday or Wednesday.[4]

### 2.2.2. Temperature effect

Outside temperatures represent another important determinant of short-term electricity demand. Temperature effects exhibit highly nonlinear features, due to different energy usage

[4] In Spain, economic activity, mainly in industry and the public sector, nearly comes to a halt in August, and hence for most Spaniards August is the typical month for summer holidays. We observe a holiday anticipation effect when the last day in July is Monday-Wednesday.

patterns when temperatures are “low” or “high”. Because temperature modifies the direction of electricity consumption or the “demand state”, i.e. if temperatures rise when temperatures are already high, consumption will increase due to the use of air condition/cooling equipment. But when temperatures are low, an increase in temperatures decreases consumption. Second, conditional on the “demand state”, changes in temperature affect electricity demand according to the “demand temperature-elasticity”. And third, calendar effects are likely to interact with the temperature effect (weekends, beginning and end of work days, holidays, etc.).

Table 1.- Type of days considered

| **Type** | **Subtype** | **Number of dummy variables** | **Cases in a year** |
|---|---|---|---|
| National holidays | weekday | 1 x 6 (1) | 8 (1) (2) |
| Regional holidays | weekday | 1 x 6 (1) | 8 (1) (2) |
| Local holidays in big cities (Madrid, Barcelona, Valencia, Sevilla, Zaragoza, Murcia) | NO | 1 x 6 (1) | 10 (1) |
| Day after national holiday | Weekday | 1x 6 (3) | 8 (3) |
| Day after regional holiday | Weekday | 1 x 6 (3) | 8 (3) |
| Christmas season (12/21 -1/7) | Weekday | 18X7 | 1x 18 |
| Easter week | 9 days | | 9 1 X 9 |
| Working days | Weekday x (Summer-not August, August and Rest) | 3 X 7 | VARIABLE |

(1) There are no holidays on Sundays.
(2) If for a given day there is a coincidence in type of days, we apply the following hierarchy: Christmas/ Easter > National > Regional > Day after national >local.
(3) As there are no holidays on Sundays, Mondays are never considered “days after” holidays.

For the case of Spain, these features are analyzed in detail by [18], among others. When dealing with high frequency data, adjusting for the temperature effect thus requires adjustments along these three dimensions. The first dimension requires estimating the threshold temperature for

which the demand behavior switches. These thresholds are determined as the average of the values that minimize the AIC criteria in the following regression:

$$E_{it} = \begin{cases} \beta_{io} + \beta_{i1} T_t + \varepsilon_{it} & T_t < \underline{\tau}_i \\ \phi_{io} + \varepsilon'_{it} & \overline{\tau}_i > T_t \geq \underline{\tau}_i \\ \theta_{io} + \theta_{i1} T_t + \varepsilon'_{it} & T_t \geq \overline{\tau}_i \end{cases} \quad \text{[eq. 7]}$$

where $E_{it}$ is the load data at hour *i* on day t from which the weekly cycle is filtered out by taking a centered moving average of 7 terms, while the trend is filtered out using a Hodrick Prescott filter. This regression also includes a month dummy to take into account the seasonality in electricity consumption that is not driven by temperature variations. The estimates are 15ºC and 20ºC for the low and high temperature thresholds respectively.

Note that these thresholds are much more related to inside comfort temperature than to observed outside temperature. Hence, outside temperatures, although related to inside temperature, do not necessarily have an immediate and contemporaneous effect on electricity demand. Given the strategy of modelling each hourly load separately, ideally it would be preferable to use hourly data for outside temperatures. However, due to the very high costs of hourly temperature data this option is disregarded. In any case, due to the inertia in inside temperatures (heat-loss is not linear as pointed out in e.g. Henley and Peirson,1997 [19]) only a limited impact for our estimates can be expected. Nevertheless, to better capture the true temperature effect, in the model specification it is also included the minimum and maximum daily temperatures together with the mean temperature[5], and a moving average temperature over five consecutive days.

The following functional form for estimating the temperature effect is hence adopted,

$$g_i(T) = g_i(T\min_t, T\min_{t-1}, \ldots T\min_{t-4,}\ T\max_t, T\max_{t-1}, \ldots T\max_{t-4,}) = \beta_{0i}(T_t < \underline{\tau}) + \beta_{1i}(T_t \geq \overline{\tau}) +$$
$$+ \beta_{2i} T_t (T_t < \underline{\tau}) + \beta_{3i} T_t (T_t \geq \overline{\tau}) + \sum_{l=1}^{4} \theta_{ij} T_{t-j} (T_{t-j} < \underline{\tau}) + \phi_{ij} T_{t-j} (T_{t-j} \geq \overline{\tau}) + \beta_{4i} R_t^3 (T_t < \underline{\tau}) + \beta_{5i} R_t^5 (T_t \geq \overline{\tau}) +$$
$$+ \beta_{6i} A_t (T_t < \underline{\tau}) + \beta_{7i} A_t (T_t \geq \overline{\tau}) + \beta_{8i} T_t^2 (T_t \geq \overline{\tau}) + \beta_{8i} T_t^2 (T_t < \underline{\tau}) + \beta_{9i} (T\max_t - \overline{\tau})(T_t > \overline{\tau}) +$$
$$+ \beta_{10i} (\underline{\tau} - T\min_t -)(T_t < \underline{\tau})$$

eq.8]

where $T_t$ is the daily mean temperature defined as $T_t = \frac{T\max_t + T\min_t}{2}$, $\underline{\tau}$ is the estimated threshold for "low temperatures" and $\overline{\tau}$ the threshold for "high temperatures". $R_t^5$ is the moving average value of mean temperatures over five consecutive days, and $A_t$ is the daily thermal

[5] The temperature used is the mean of the minimum and maximum temperatures on a given day. Minimum and maximum temperatures are the weighted average of temperatures recorded at seven observatories (Málaga, Bilbao, Barcelona, Madrid, Valencia, Sevilla and Valladolid). These observatories are representative of the climatological areas in Spain. Our weights are given by the share in electricity consumption of each area.

amplitude.[6] To deal with nonlinearities in the demand-temperature elasticity, also a quadratic temperature as an additional explanatory variable is included.

The proposed model for the temperature effect allows for different temperature elasticities depending on the hour of the day and the type of day considered, as well as depending on the "history" of temperatures (i.e., the previous four day values). The interaction of the working day effect and the temperature effect introduces a highly nonlinear behavior[7] into electricity demand. Figure 5 shows that the observed effect on electricity demand of a decrease in outside temperatures by 1ºC ranges from 580 MWh to 153 MWh measured at 8 pm in the winter and from 776MWh to 607 MWh measured at 1 pm during the summer. Furthermore, independently of the season, a much higher variability in the temperature effect at 1 pm than at 8 pm can be observed.

**Figure 5.- Electricity demand at 1 pm and 8 pm vs outside temperatures (daily data 2001-2014).**

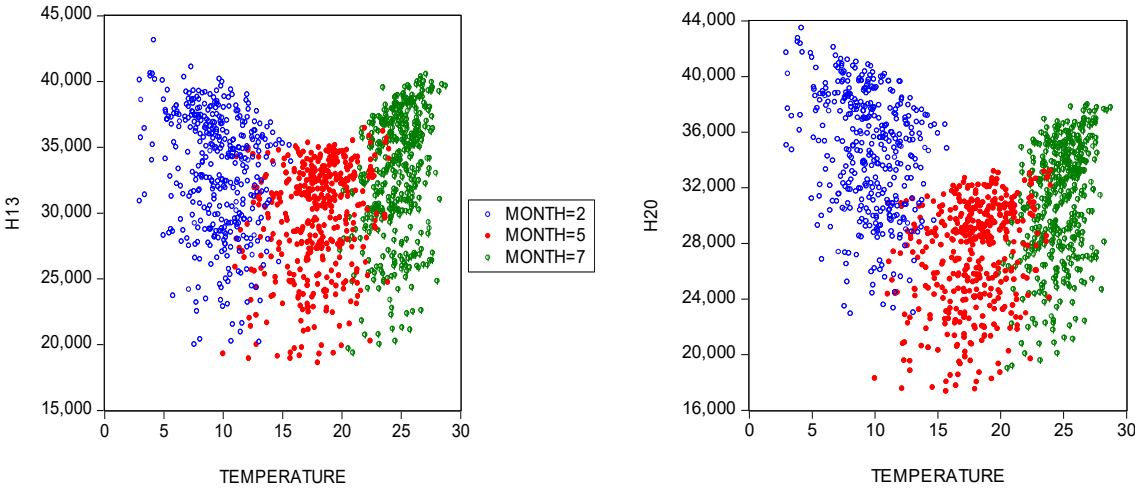


Note: Data for electricity load is raw data. The theoretical temperature effect is u-shaped but the long-term trend and the weekday effect are such that they displace, both upwards and downwards, the theoretical u-shape response to temperature.

---

[6] The difference between maximum and minimum temperatures on a given day; i.e. $A_t = T\max_t - T\min_t$.

[7] Non-linearity in the demand elasticity to temperature variation can be also derived within our theoretical model:

$$\frac{\partial g_i(tempe_t)}{\partial T\min} = \begin{cases} \frac{1}{2}\beta_{2i} + \frac{1}{2}\sum_{l=1}^{4}\theta_{ij} + \frac{1}{2}\beta_{4i} - \beta_{6i} + \beta_{9i}T_t - \beta_{10i} & T_t < \underline{\tau} \\ \frac{1}{2}\beta_{3i} + \frac{1}{2}\sum_{l=1}^{4}\phi_{ij} + \frac{1}{2}\beta_{5i} - \beta_{7i} + \beta_{8i}T_t & T_t \geq \underline{\tau} \end{cases}$$

$$\frac{\partial g_i(tempe_t)}{\partial T\max} = \begin{cases} \frac{1}{2}\beta_{2i} + \frac{1}{2}\sum_{l=1}^{4}\theta_{ij} + \frac{1}{2}\beta_{4i} + \beta_{6i} + \beta_{9i}T_t & T_t < \underline{\tau} \\ \frac{1}{2}\beta_{3i} + \frac{1}{2}\sum_{l=1}^{4}\phi_{ij} + \frac{1}{2}\beta_{5i} + \beta_{7i} + \beta_{8i}T_t & T_t \geq \underline{\tau} \end{cases}$$

Source: Own elaboration with data from REE (Red Eléctrica de España S.A)

### 2.2.3. Daylight effect

Finally, one particularly interesting feature of electricity demand can be extracted from the analysis of differences in temperature elasticity at adjacent hours. Looking at the estimated coefficients assigned to temperatures in Equation 7 we observe certain "abnormalities" at 8-9 am and notably at 7-9 pm are observed. The estimated coefficients for the effect of outside temperatures on electricity demand are abnormally low in the "cooling" regime (high temperatures), and abnormally high in the "heating" regime (low temperatures). A plausible conjecture is that this is caused by the interaction between daylight duration and daily working hours (commercial sector opening hours, industrial activity, etc.); see Section A of the Appendix for an empirical test of this interaction. In Spain, during some months there is daylight at 6-8 am and 7-9 pm, while this is not the case during other months. Electricity demand does hence not only reflect the effects of temperatures but also lighting needs.

Lighting represents one of the original uses of electricity and its use is most clearly observed at night. Lighting use is expected to change only with the evolution of the surface to be illuminated (new homes, new commercial and industrial facilities, urban sprawl, etc.) or lighting technology (incandescent, fluorescent, LED, etc.) which determines the intensity of consumption. Such long-term effects are picked up by our low-frequency component, and there are no perceptible high frequency effects, except for electricity loads at hours for which there is a day/night transition throughout the year; i.e. 6-8 am and 7-9 pm for the case of Spain. These high frequency effects are particularly visible around daylight saving time clock shifts. The clock shift imposes a sudden change in the official time causing a displacement in the shape of the load curve, precisely at 7-8 pm (+1hour and -1 hour), and 8-9 am (-1 hour); see Figure 6. The high frequency component thus has to include this effect. Furthermore, the relationship between temperature, thermal amplitude, and daylight duration shows that the model also has to account for the interaction of daylight duration with the temperature effect.

**Figure 6 .- Changes in load curve after daylight saving time clock shifts on last Sunday in March (+1h) and October (-1h).**

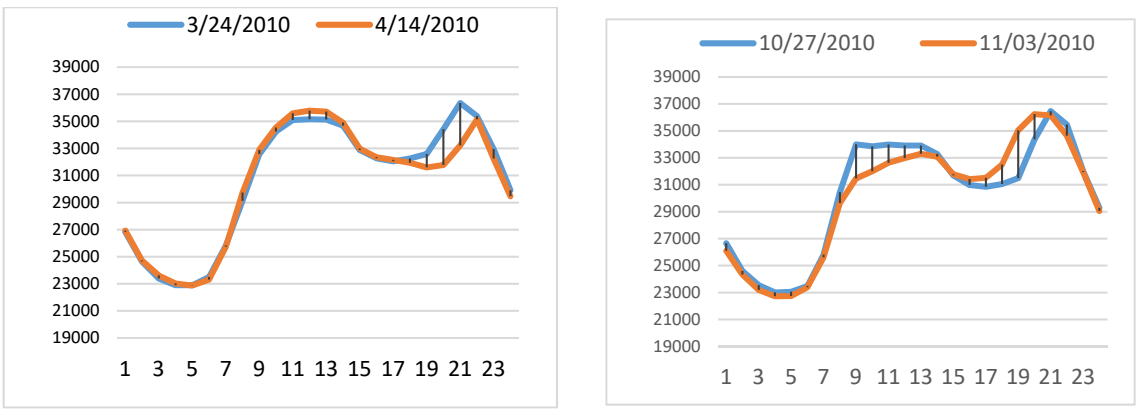

Source: Own elaboration with data from REE (Red Eléctrica de España S.A)

## 2.3 MODEL FOR HOURLY DEMAND

The proposed procedure requires to analyze each hourly data of the load curve independently. In particular, the observed electricity consumption at a given hour *i* is assumed to be the result of a long-term component, $LF_t$ plus a high frequency component, $HF_t$ which is linked to calendar and temperature effects. The following specification for hourly demand is proposed:

$$c_{it} = \varphi_i(LF_t, HF_t) + \varepsilon_{1,t} = h_i(LF_t) + f_i(D_t) + g_i(T_t) + \varepsilon_{i,t} \quad \text{[eq.9]}$$

where $c_{it}$ is hour *i*'s mean load power on day *t* and $f_i$ (),is the calendar effect, $g_i$ (), is the temperature effect, and $LF_t$ is the low-frequency component for hour *i* on day *t.* The model parameters are estimated by minimizing the sum of the squared errors in eq.9, that is , minimizing the expression, $Min \sum_{t=1}^{T}[c_{i,t} - \varphi_i(LF_t, HF_t)]^2$-

The low frequency component is specified as follows:

$$h_i(LF_t) = \omega_i C_t, \quad \text{[eq.10]}$$

where $C_t$ is the value of the historical/forecasted annual demand disaggregated on a daily basis using the BFL method as previously discussed.

For hours 7- 8 am and 7-9 pm, Equation 9 also includes as an additional explanatory variable the time of sunrise ( $Sr_t$ ) and sunset ( $Ss_t$ ) to account for the impact of daylight duration on lighting demand:

$$m_i(S_t) = \begin{cases} \theta_{1i}(Sr_t \geq i) + \theta_{i2} Sr_t(Sr_t \geq i) & i = 7,8 \\ \theta_{1i}(Ss_t < i-1) + \theta_{2i}(Ss_t > i) + \theta_{i2} Ss_t(Ss_t < i-1) & i = 19,20,21 \end{cases} \quad \text{[eq.11]}$$

The same specification is considered for all hours (with the obvious exception of the $m_i(S_t)$ component specified in Equation 11). Disposable data cover the period 1/1/1996- 12/31/2014, and hence for each hour more than 6,900 daily observations of hourly electricity load are available to estimate 219/216 coefficients (on days when the daylight saving time clock shift

occurs observations for 3 am are excluded ). As an example, in section B of the Appendix our full estimation results for 8 pm are detailed.

# 3. MODEL PERFORMANCE

The model performs well in terms of fit as measured by the hourly R-squared coefficient, especially around peak hours (7-8 pm in the winter and 1-2 pm in the summer). For low activity periods, like 1 -7 am, the R-squared coefficient lies somewhat below 0.97. The correlation of the residuals is linked to the weekly cycle, and the structure of the correlation across equations suggests that this effect is stronger for adjacent hours and that it becomes very weak for distant hours; for the evolution of the residuals over time see Figure A2 of the Appendix. For all cases, the correlation diminishes with the length of the time period considered, and it only remains significant due to the weekly cycle.

## 3.1 MODEL FORECASTING PERFORMANCE

Given the forecasting purpose of our model, first its accuracy for replicating the data is analyzed. This test is intended to validate the accuracy and stability of the model. To this end, the model is estimated recursively with moving samples, including one more year of observations at a time, and then launching predictions to 12/31/2014 (last available data point). The incurred errors are checked at each estimation-forecasting stage, first using data up to 2010[8], and then adding one year of data at a time. At each stage, the forecasting period is shortened. At the first stage (estimation period 1996-2010) we analyze four years of daily data, and at the last stage, seven years of daily data (estimation period 1996-2013). As measures of accuracy the mean absolute error (MAE) and the percentage mean error (PMEA) are computed (Table 2):

$$MAE = \frac{1}{T}\sum \left| c_{i,t} - \hat{c}_{it} \right|$$

MAE , Mean absolute error , [eq.12]

$$MAPE = \frac{1}{T}\sum \frac{\left\| c_{i,t} - \hat{c}_{it} \right\|}{c_{i,t}}$$

MAPE, Mean absolute percentage error , [eq.13]

where $c_{i,t}$ denotes the actual value of electricity load at hour *i* on day *t*, and $\hat{c}_{it}$ is the estimated variable.Both measures are calculated for each of the four following cases: **2010** (estimation: 1996-2010, prediction: 1/1/2011-12/31/2014); **2011** (estimation: 1996-2011, prediction:

[8] The model estimated with data from 1996-2010 and forecasted from 1/1/2011 onwards is particularly interesting as it allows to see the advantages of this method in comparison to the alternative method of extracting the underlying trend using the Hodrick-Prescott Filter and forecasting it. If the HP filtered series is modelled as an IMA(2,1) process, the forecasted values remains nearly constant. Other models for the HP filtered values, like the IMA(1,2) perform even worse as forecasts show an upward trend while the observed pattern was a decreasing trend due to the "double-dip" recession experienced by the Spanish economy.

1/1/2012-12/31/2014); 2012 (estimation: 1996-2012, prediction: 1/1/2013-12/31/2014); and 2013 (estimation: 1996-2013, prediction: 1/1 /2014-12/31/2014).

Table 2.- Measures of model's accuracy: MAE and MAPE values for each estimated equation Hi (i:1,…,24)

**MAE**

| | H1 | H2 | H3 | H4 | H5 | H6 | H7 | H8 | H9 | H10 | H11 | H12 | H13 | H14 | H15 | H16 | H17 | H18 | H19 | H20 | H21 | H22 | H23 | H24 |
|---|---|---|---|---|---|---|---|---|---|---|---|---|---|---|---|---|---|---|---|---|---|---|---|---|
| 2010 | 942.0 | 848.8 | 845.3 | 647.2 | 560.9 | 508.5 | 532.0 | 813.1 | 937.3 | 962.8 | 896.6 | 883.6 | 843.2 | 857.0 | 931.9 | 861.4 | 904.6 | 1,002.1 | 1,058.7 | 905.0 | 734.6 | 648.6 | 670.0 | 930.7 |
| 2011 | 944.2 | 841.8 | 836.0 | 635.2 | 548.6 | 487.4 | 497.7 | 745.0 | 885.8 | 937.1 | 895.7 | 897.0 | 848.7 | 823.7 | 865.9 | 835.9 | 907.7 | 1,024.0 | 1,066.9 | 905.5 | 718.0 | 628.0 | 658.1 | 974.7 |
| 2012 | 884.1 | 762.6 | 758.0 | 565.9 | 487.7 | 446.2 | 463.7 | 703.9 | 856.2 | 922.7 | 910.4 | 918.7 | 869.2 | 827.1 | 851.8 | 828.6 | 899.0 | 1,024.9 | 1,065.9 | 902.8 | 699.8 | 616.1 | 664.7 | 972.2 |
| 2013 | 776.8 | 668.8 | 683.6 | 516.8 | 468.6 | 469.9 | 503.8 | 719.2 | 879.7 | 937.0 | 932.2 | 939.8 | 886.7 | 807.3 | 810.1 | 816.0 | 896.9 | 1,014.6 | 1,036.1 | 878.4 | 680.1 | 600.0 | 641.9 | 912.9 |

**MAPE**

| | H1 | H2 | H3 | H4 | H5 | H6 | H7 | H8 | H9 | H10 | H11 | H12 | H13 | H14 | H15 | H16 | H17 | H18 | H19 | H20 | H21 | H22 | H23 | H24 |
|---|---|---|---|---|---|---|---|---|---|---|---|---|---|---|---|---|---|---|---|---|---|---|---|---|
| 2010 | 3.58% | 3.49% | 3.33% | 2.90% | 2.55% | 2.29% | 2.26% | 3.12% | 3.41% | 3.35% | 3.00% | 2.89% | 2.73% | 2.75% | 3.05% | 2.91% | 3.08% | 3.38% | 3.46% | 2.91% | 2.33% | 2.00% | 2.18% | 3.27% |
| 2011 | 3.61% | 3.48% | 3.31% | 2.86% | 2.51% | 2.21% | 2.14% | 2.89% | 3.27% | 3.30% | 3.03% | 2.96% | 2.77% | 2.67% | 2.86% | 2.85% | 3.11% | 3.46% | 3.50% | 2.93% | 2.29% | 1.97% | 2.18% | 3.45% |
| 2012 | 3.40% | 3.17% | 2.99% | 2.56% | 2.23% | 2.04% | 2.01% | 2.77% | 3.21% | 3.30% | 3.10% | 3.05% | 2.85% | 2.70% | 2.84% | 2.84% | 3.10% | 3.49% | 3.52% | 2.93% | 2.25% | 1.96% | 2.23% | 3.47% |
| 2013 | 3.02% | 2.79% | 2.65% | 2.33% | 2.14% | 2.13% | 2.17% | 2.85% | 3.33% | 3.38% | 3.20% | 3.13% | 2.91% | 2.64% | 2.70% | 2.80% | 3.10% | 3.47% | 3.44% | 2.88% | 2.20% | 1.93% | 2.18% | 3.30% |

The average absolute error lies below 1100 MWh whether the forecast horizon is long or short, representing less than 4% of electricity load, see Table 2. This can be interpreted as a sign of stability of the estimated model. The errors are particularly low during peak hours, at 8-10 pm and 1-2 pm, while the worst results are obtained for hours characterized by relatively low consumption; i.e. between 11 pm and 4 am.

### 3.1.1. Analysis of forecasting performance

In this section we compare the forecasting performance of the model presented in the previous section, hereafter model LFC+HFC (low frequency component + high frequency component), with the results obtained using a nonlinear autoregressive neural network with exogenous inputs (NARX model). This kind of model is suitable for the type of problem analyzed here given the flexibility of the Artificial Neural Networks (ANN's) which allows to capture typical nonlinearities in the load curve caused by the working day cycle and temperature effect in electricity demand. Next to a number of exogenous variables, the ANN uses lagged values of the load curve as inputs which allows the model to capture the trend in the load curve; see Figure 7. We also consider an alternative version where additionally a quadratic time trend is included as an input variable.

The NARX model with three layers that it is considered as a comparison model, has the following specification,

$$c_{i,t} = \sum_j^{ni} w_j^i \left[ f\left( \sum_k^{nx} w_{j,k}^i \, x_{k,t}^i + \sum_{l=1}^{nl} w_{j,l}^i \, c_{i,t-l} \right) \right] + e_{i,t} \quad , \quad \text{[eq.14]}$$

where $c_{i,t}$ is the electricity load at hour i on day t, $c_{i,t-l}$ are the *l* day lagged value of electricity load at hour i, and $x_{k,t}^i$ are the values of the $nx$ exogenous variables used to explain the load at hour i on day t. The hidden layer has $ni$ neurons, and each neuron has $nx$ inputs or exogenous variables, and $nl$ lags of the output variable with weights $w_{j,k}^i$, and $w_{j,l}^i$ respectively. The hidden layer employs a sigmoid transfer function from inputs to output, and at each output layer it uses a linear transfer function with weights $w_j^i$. Finally, $e_{i,t}$ is the error term, i.e. the difference between the true value of electricity load and the estimated output of the NARX model.

The exogenous variables used in the NARX model are the same as the ones in the high frequency component of the LFC+HFC proposed model[9], including variables for the calendar effect and monthly seasonality (193 variables), variables for the temperature effect (21 variables) and variables for the daylight effect (only for 6-8 am and 7-9 pm). Therefore, as inputs a total of $nx$ =217 exogenous variables are included, plus the lagged values of the load curve at hour $i$. This selection of variables is similar to those used by [4] who employ a deep belief network, but in addition for the NARX model here more detailed calendar and temperature effects are used.[10]

[9] See the appendix for a detailed enumeration of the variables.

[10] In Dedinec et al 2016 [4] input variables are the hour of the day, the day of the week, holiday indicator, average load on previous day, load for the same hour on previous day, temperature, a cheap tariff indicator, and the load at the same hour and day of week in the previous week.

As mentioned before, an alternative version of the model that also includes quadratic trend terms as input variables to better capture the long term evolution of the load curve is considered as well. In this case the number of exogenous input variables increases to $nx$ =219.

Figure. 7- Schematic representation of the NARX model

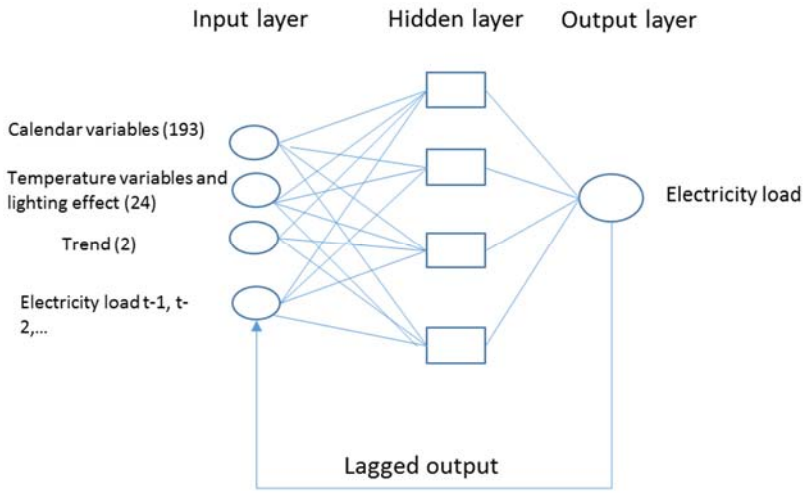


Source: Own elaboration

To determine the number of hidden units, $ni$, and the number of output lags, $nl$, a "*brute-force*" procedure is applied. To this end NARX models with different values of $ni$ and $nl$ from intervals [1,15] and [1,14] respectively are trained and tested, retaining the value of the "optimal"[11] MSE (mean squared error) for the NARX($ni, nl$) model in the test sample. Finally, $ni$ and $nl$ are chosen from the NARX($ni, nl$) models with the lowest value of the MSE for each of the different specifications analyzed, see Table 2. It is important to point out that while for the NARX(ni,nl) with quadratic trends a total of [ni x (219+nl)] coefficients (weights) have to be computed, in the LFC+HFC model only 218 coefficients need to be estimated.

To compare the performance of the LFC+HFC model to the different specifications of the NARX model, the load data at 8 pm, which concentrates the highest frequency of annual peak loads, are used. The LFC+HFC model is estimated for the 1996-2010 period and daily predictions are made for 2011-2014(1461 values). The NARX model is trained with data for the same period, and forecasts are launched for 2011-2014 under two distinct scenarios. A "real-world" scenario, where a closed loop version of the NARX model is considered (i.e. the lagged electricity loads used as inputs are the predicted values of the electricity load, allowing for forecasts along the entire

[11]For each hour the total sample size is 5,479 (daily data from 1/1/1996 to 12/31/2010). The NARX model is trained with 3.835 data points, validated with 822 data points, and tested with 822 randomly selected data points. "Optimal" MSE refers to the value of the MSE in the epoch with the lowest value of the MSE of the trained NARX model in the selection sample.

horizon), and an "optimal fit" case where an open loop version of the NARX model is employed (i.e. the lagged electricity load used as inputs are the true values of the electricity load, only allowing for one-day-ahead forecasts). As performance measures the MAPE and the MSE are calculated, see Table 3. The results show that the LFC+HFC model performs well, with a MAPE value similar to the one from an open-loop version of the NARX model. In comparison to the closed loop version, more realistic in terms of a real-world forecasting exercise, the performance of the LFC+HFC model is clearly superior.

Table 3.- Comparative values of performance measures.

| | MAPE | | MSE | |
|---|---|---|---|---|
| **Model LFC+HFC** | 2.8% | | 1,235,618 | |
| **NARX with quadratic trend** | Closed Loop | Open Loop | Closed Loop | Open Loop |
| $ni$=10, $nl$ =11 | 3.7% | 2.4% | 2,293,174 | 1,201,633 |
| $ni$=8, $nl$ =11 | 7.0% | 2.9% | 7,735,151 | 1,677,151 |
| $ni$ =1, $nl$ =13 | 4.2% | 2.4% | 4,006,233 | 1,947,101 |
| **NARX without trend** | Closed Loop | Open Loop | Closed Loop | Open Loop |
| $ni$ =10, $nl$ =11 | 16.3% | 2.9% | 35,766,888 | 1,656,525 |
| $ni$ =5, $nl$ =11 | 27.9% | 3.3% | 97,130,977 | 1,757,538 |
| $ni$ =2, $nl$ =12 | 7.7% | 3.0% | 8,334,711 | 2,455,380 |

Note: Model LFC+HFC (low frequency component + high frequency component) is the model detailed in the paper. Only in the NARX models with the quadratic trend terms the error autocorrelation is not significant. In the NARX model with no trend the autocorrelation in residuals induce persistent deviations from the true values of electricity load, which could explain why the MAPE error in the closed loop version is so high.

### 3.1.2. Extreme values forecasting performance

The methodology presented in this paper is oriented towards long-term peak and trough load forecasting. The modelling approach allows us to obtain hourly load estimates whose accuracy can be tested in several ways. The most obvious test is to graphically compare the observed and the projected values for hourly load forecasts. But given that both accuracy measures (MAE and PMEA) are low it can be expected that both values move together; see Figure 8.

Figure. 8- Hourly load forecast and actual values. 2014


Note: The estimation period is 1996-2010 and the forecast horizon 2011-2014 (1461 predictions for each of the 24 series). We only show values for 2014.

A more interesting test in line with the objective of the paper is to determine the ability of the model to predict extreme values, such as the minimum and maximum load values in a given period (e.g. a month). This type of analysis can be approached in two ways: (i) Simply comparing the true observed extreme values and the predicted ones[12]. (ii) Visualizing the ability of the model to reproduce the observed frequencies of load values; i.e. constructing a histogram or probability density of load values. The latter provides a measure of confidence regarding the accuracy of the model. In a realistic forecasting environment when deciding which model to use for simulating different scenarios of temperatures and long-term demand situations this is a very useful

[12] We compare the observed monthly extreme values (highest and lowest load data) with the ones predicted by the model for the same day (estimation with data until 2010 and forecasting from 2011 to 2014). To make predictions we use "true" temperature values and long-term demand projections. The prediction error lies between [-3618 / 1371] GWh (on average 2.8%), with underestimation (estimated value less than the actual value) prevailing. If we analyze annual extreme values, the estimation error in the prediction period is below 3.0% for peaks, and 3.3% for troughs.

measure. From the so-constructed histogram it can be immediately observed that the actual critical values - "value-at-risk" - of electricity demand; i.e. values of demand that will not be exceeded at a given level of probability. This result has direct practical applications for grid and generation long-term planning.

In Figure 9 we show the probability density function estimated from the histogram of load data (probability of obtaining a given value) with observed and forecasted values up to 2014, using the model estimated with data from 1996 to 2010. In global terms the model performs well, reproducing the bi-modal distribution of load values (the Kullback-Leibler divergence measure is 0.65*10^(-4) ). For load values at the bottom half of the distribution the predicted values are shifted towards lower values, i.e. the model assigns a higher probability to lower values than are observed. This pattern is especially visible for January and December as well as for September. However, while this weakness of the model should be taken into account, this is not an important limitation given that the main aim of the model is to help. In this context the maximum load is much more critical than its minimum value.

4. **Figure 9.- Probability density function for load values. 2014. Actual and predicted values.**

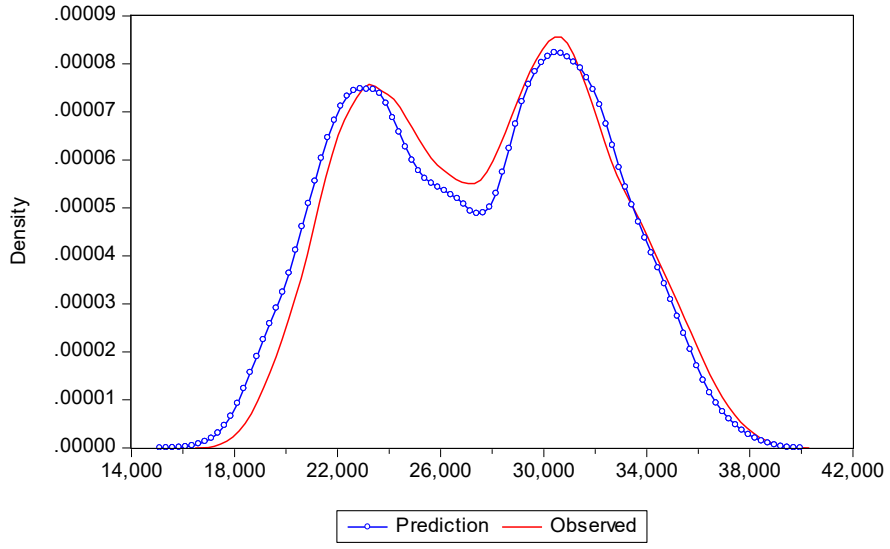


5.
6. Note: Kernel estimation Epanechnikov method.
7. Source: Own elaboration.

## 7.1. LONG-TERM SIMULATION

Once the goodness of fit of the model has been established, the model can be incorporated into the simulation process. A flow chart for such a simulation process is represented in Figure 10. The starting point is the definition of a macroeconomic scenario which is translated into alternative annual growth scenarios for electricity demand. These annual values are then converted into daily values via the described BFL methodology. The high frequency components (calendar and temperature effects) are then incorporated into the simulation process in two different ways: Calendar effects (calendar days, holidays, month dummies, sunrise and sunset times) are nearly

deterministic and are considered as fixed across alternative simulations. Temperature effects are random and are simulated using Monte Carlo trials[13]. For each trial the extreme values of interest are retained (annual maximum and minimum loads, maximum loads in winter and summer, monthly maximum, etc.).

Figure 10- Simulation flow chart

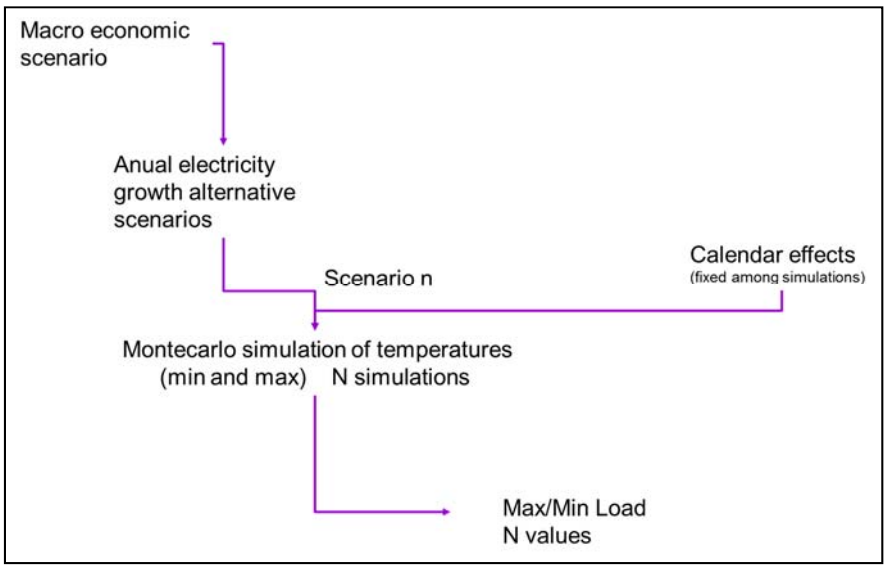


Source: Own elaboration.

As an example for the proposed simulation process, in Figure 11 the simulated peak loads for 2020 are presented, assuming that electricity demand grows at an annual rate of 1.6% during 2015-2020. In the simulation, 3000 Monte Carlo trials for temperature are used, and 3000 alternative hourly load forecasts are computed. Then the 3000 peak values for winter and summer are retained. As it can be observed, both winter and summer peak loads are skewed to the right with larger right tails, showing that extremely unfavorable (and unlikely) scenarios for temperatures can cause huge increases in peak loads. Coherent with the long-term evolution of electricity demand, this kind of analysis allows to assign probabilities to different values of peak loads, and to thus establish security margins for the electricity grid.

[13] The model used to simulate temperatures is the following

$$T_t = \phi T_{t-1} + v_t$$

$$v_t = \mu_i + \varepsilon_{it} \qquad i = 1,2,.....,24$$

where $T_t$ is the temperature variable (daily minimum or maximum temperature), $\mu_i$ is the intercept value of the temperature variable (daily minimum or maximum observed in the $i$=1,2,…,24 bi-weekly period (sample 1/1/1996-12/31/2014). $\phi$ is the persistence parameter which is estimated via OLS as is the residual term $\varepsilon_{it}$ . For simulation purposes the estimated residual is assumed to be normally distributed with mean zero and standard deviation equal to the one computed from the residual terms $\varepsilon_{it}$ . In each trial a realization of $\varepsilon_{it}$ is generated for the prediction range. The advantage of this method is that it allows to capture both the observed persistence in temperatures (the parameter $\phi$ ) and the intra-year observed pattern (increasing from January to August and then decreasing, with higher volatility in the winter).

8. Figure 11.- Simulation of peak load for the summer and winter, forecasts for year 2020 assuming 1.6% annual growth rate for electricity demand.

a) Winter peak load

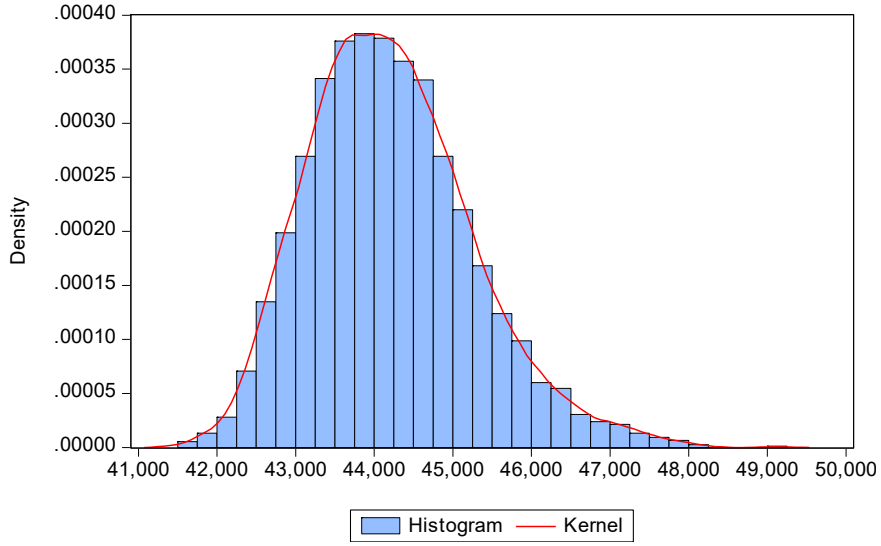


b) Summer peak load.

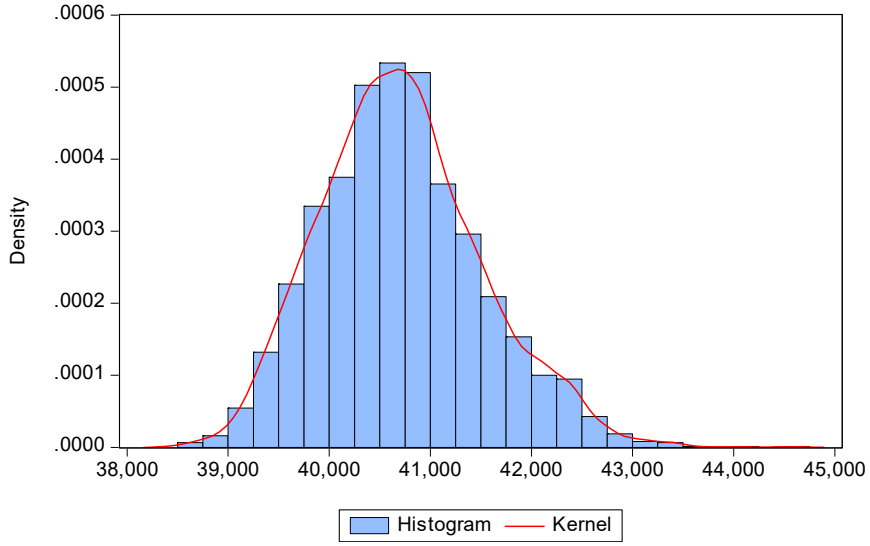


Source: Own elaboration.

# 9. CONCLUSIONS

Long-term peak load forecasting requires to deal with both high and low frequency or trend components. When forecasting high frequency variables, like daily or hourly loads, the way trend components are treated is critical because long-term scenarios have to be made compatible with short term projections. The forecasting procedure has to be flexible enough to allow simulating alternative long-term scenarios that usually come from other models, or from different policy objectives, or are simply "what if" simulations. In this paper, a novel forecasting procedure is proposed using causal models which combines long and short-term features by employing temporal disaggregation techniques. The procedure is flexible enough to analyze different

scenarios based on alternative assumptions regarding both long-term trends as well as changes in high frequency components.

The main advantage of this procedure is that it allows to control for long-term developments like changes in GDP growth, demographic variables, and technological progress. Technically, the use of the Boot Feibes and Lisman (BFL) procedure is proposed, a well-known methodology for temporal disaggregation. Using the BFL procedure, the outcome of long-term models can be used for forecasting because it allows to deal with low frequency component in hourly loads. At the same time, the modelling approach proposed is able to include high frequency components such as calendar or temperature effects. Daylight duration is also included, a variable that has not been employed much in the literature. This variable only matters at certain hours, but in the case of Spain these are precisely the hours when peak loads occur (7-9pm).

The model's performance is tested using historical data, with an average absolute error below 1100 MWh, which represents less than 4% of the hourly electricity load. The estimation errors are especially low for peak hours (8-10 pm and 1-2 pm), while the worst results are achieved during hours characterized by relatively low consumption of electricity (between 11 pm and 4 am).

The ability of the model to reproduce the observed frequency of load values is also tested i.e. the histogram or probability density of load values. This analysis is crucial in order to assign probability levels to load range forecasts. In global terms the model performs well, reproducing the bi-modal distribution of load values in Spain (the Kullback-Leibler divergence measure is 0.65*10^(-4) ). For load values at the bottom half of the distribution the model assign higher probabilities to lower values than are truly observed (especially visible in January, December and September). This weakness is not very limiting given the aim of the model to help in grid capacity planning where the maximum load is much more critical than its minimum value.

## ACKNOWLEDGEMENTS

The authors are grateful to Red Eléctrica de España S.A for their financial support in developing this project and providing the data needed. We also benefited from comments by Almudena Carrasco-Reija and David Alvira-Baeza from the Electrical Planning Department of Red Eléctrica de España S.A. We also thank Zoe Kuehn for her valuable comments and suggestions. Naturally, the authors remain solely responsible for any errors or omissions.

# REFERENCES

[1.] Che, J. and Wang, J. Short-term load forecasting using a kernel-based support vector regression combination model. Applied Energy. 2014, 132, 602-609.

[2.] Yang, Y., Che, J. m Li, Y,, Zhao, Y., and Zhu, S. An incremental electric load forecasting model based on support vector regression. Energy, 2016, 113, 796-808.

[3.] Che, J. A novel hybrid model for bi-objective short term electric load forecasting. Electrical Power and Energy Systems. 2014, 61, 259-266.

[4.] Dedinec, A., Filiposka, S., Dedinec, A., and Kocarev, L. Deep belief network based electricity load forecasting: An analysis of Macedonian case. Energy. 2016. 115 , 1688-1700
[5.] Badurally Adam, N.R., Elahee, M.K. and Dauhoo M.Z. Forecasting of peak electricity demand in Mauritius using the non-homogeneous Gompertz diffusion process. Energy. 2011, 36, 6763-6769.
[6.] Hahn, H., Meyer-Nieberg, S.,and Pickl, S. Electric load forecasting methods: Tools for decision making. European Journal of Operational Research.2009, 199, 902–907.
[7.] Zhao, H. and Guo, S. An optimized grey model for annual power load forecasting. Energy, 2016, 107, 272-286.
[8.] Nedellec, R., Cugliari, J., and Goudea, Y. GEFCom2012: Electric load forecasting and backcasting with semi-parametric models. International Journal of Forecasting.2014. 30; 375–381.
[9.] Taylor, J W. Triple seasonal methods for short-term electricity demand forecasting. European Journal of Operational Research.2010, 204,139-152.
[10.] Mestekemper, T, Kauermann, G. and Smith, M.S. A comparison of periodic autoregressive and dynamic factor models in intraday energy demand forecasting. International Journal of Forecasting, 2013, 29, 1-12.
[11.] Bianco, O. Manca, S. Nardini. Linear regression models to forecast electricity consumption in Italy Energy Sources Part B. 2013, 8, 86–93.
[12.]Cho, H., Goude, Y., Brossat, X., and Yao, Q. Modelling and forecasting daily electricity load curves: a hybrid approach. Journal of the American Statistical Association.2013, 108; 7–21.
[13.]Hyndman, R.J, and Fan, S. Density forecasting for long-term peak electricity demand. EEE Transactions on Power Systems, 2010, 25, 1142-1153.
[14.]Soares, L. J. and Medeiros, M. C. Forecasting electricity demand using generalized long memory. International Journal of Forecasting, 2006. 22, 17–28.
[15.]Pérez-García, J. and Moral-Carcedo, J. Analysis and long term forecasting of electricity demand trough a decomposition model: A case study for Spain. Energy. 2016, 97, 127–143.
[16.]Boot, J., Feibes, W., Lisman, J. Further Methods of Derivation of Quarterly Figures from Annual Data. Applied Statistics.1967.16, 65 75.
[17.]Moral-Carcedo, J., and Vicéns-Otero, J. Modelling the non-linear response of Spanish electricity demand to temperature variations. Energy Economics, 2005 27, 3, 477-494
[18.]Moral-Carcedo, J. and Pérez-García, J. Temperature effects on firms' electricity demand: An analysis of sectorial differences in Spain. Applied Energy, 2015, 142 407–425
[19.]Henley, A., and Peirson, J. Non-Linearities in Electricity Demand and Temperature: Parametric Versus Non-Parametric Methods. Oxford Bulletin of Economics & Statistics,1997, 59, 149-162 .